



1

2

3

Estimating CO₂ Emissions for 108,000 European Cities

4

5 **Authors:** Daniel Moran^{1,*}, Peter-Paul Pichler², Heran Zheng¹, Helene Muri¹, Jan Klenner¹, Diogo
6 Kramel¹, Johannes Töbбен², Helga Weisz², Thomas Wiedmann⁴, Annemie Wykmans⁵, Anders Hammer
7 Strømman¹, Kevin R. Gurney⁶

8

9 Affiliations:

- 10 1. Programme for Industrial Ecology, Department of Energy and process Technology, Norwegian University of Science and
11 Technology, Trondheim, Norway
12 2. Potsdam Institute for Climate Change Research (PIK), Potsdam, Germany
13 4. Sustainability Assessment Program, School of Civil and Environmental Engineering, UNSW Sydney, Australia
14 5. Faculty for Architecture and Design, Norwegian University of Science and Technology, Trondheim, Norway
15 6. School of Informatics, Computing, and Cyber Systems, Northern Arizona University, Flagstaff, AZ, USA

16 * Corresponding author: daniel.moran@ntnu.no

17

18 Abstract

19
20 City-level CO₂ emissions inventories are foundational for supporting the EU's decarbonization goals.
21 Inventories are essential for priority setting and for estimating impacts from the decarbonization
22 transition. Here we present a new CO₂ emissions inventory for 116,572 municipal and local
23 government units in Europe. The inventory spatially disaggregates the national reported emissions,
24 using 9 spatialization methods to distribute the 167 line items detailed in the UN's Common Reporting
25 Framework. The novel contribution of this model is that results are provided per administrative
26 jurisdiction at multiple administrative levels using a new spatialization approach. All data from this
27 study is available along with an interactive map of results at <https://openhgmap.net>

28

29 1. Background

30 While climate goals are set at the national and international level it is often local governments and
31 citizens who are most intimately involved in the accomplishment of these goals, and who must adapt
32 to the implied changes. The European Commission has been clear that cities will play a central role in
33 reaching European climate goals. As with nation-states, a greenhouse gas (GHG) inventory is the first
34 step to preparing a local climate action plan (CAP). Cities often use one of the various protocols
35 available or develop their own methodology to create an emissions inventory. And for good reason -
36 an inventory informs all levels of municipal decision making, from long-term planning strategies to
37 infrastructure investments and day-to-day management of building permits. Nevertheless, many local
38 governments in Europe still do not have a good estimate of their own GHG emissions. Establishing an
39 emissions inventory is laborious and can be costly for jurisdictions that do not have in-house expertise.
40 Hence, as the spotlight turns to cities to effect and manage a successful transition to carbon neutrality,
41 many see the preparation and maintenance of a local emissions inventory as a considerable challenge.

42 Cities can develop their own inventories using a protocol such Global Protocol for Community-Scale
43 Greenhouse Gas Emissions Inventories (Fong et al., 2016) a joint initiative of WRI, the C40 Global
44 Covenant of Mayors, and ICLEI (Kona et al., 2021). An inventory informs all levels of municipal decision
45 making, from long-term planning strategies to infrastructure investments and day-to-day
46 management of building permits.



47 A number of GHG monitoring, reporting, and verification (MRV) solutions have been put forward.
48 These include sensor networks (both ground and space-based), and a range of accounting and model-
49 based approaches. No one of these approaches is ideal: they differ in terms of accuracy, precision,
50 cost, and scalability. In response it has therefore been suggested that MRV efforts should aim at
51 triangulating true CO₂ emissions using a mix of empirical, modeling, and statistical methods (Lauvaux
52 et al., 2020; Mallia et al., 2020). The model presented here should be seen as one estimate, to be
53 combined with other estimation approaches and local knowledge, to triangulate towards an
54 actionable emissions inventory.

55 One approach for cities to monitor emissions is by using atmospheric measurement of GHG
56 concentrations and “inverting” that for an emission quantity. These efforts require atmospheric
57 transport models to translate the atmospheric mixing ratios into surface fluxes of GHGs (Davis et al.,
58 2017; Ghosh et al., 2021). Concentration measurements can include dense, low-cost sensors (Kim et
59 al., 2018), high-precision tower-mounted instruments (Turnbull et al., 2019; Whetstone, 2018),
60 aircraft and satellite-based measurements (Nasa, 2021; Jaxa, 2021; Wu et al., 2020) and/or
61 combinations of all of the above. By combining these approaches with high-resolution emission data
62 products built using bottom-up approaches, attribution to emitting source by sector or fuel is possible
63 and has shown good convergence (Basu et al., 2020; Lauvaux et al., 2020; Mueller et al., 2021)

64 Many estimates of emissions using techniques independent of atmospheric monitoring have also been
65 accomplished. These inventory approaches are often described as being either “top-down” or
66 “bottom-up” (though in fact models may use a combination of these approaches). Top-down models
67 begin from national statistics, such as national energy use or fuel import statistics, while bottom-up
68 approaches estimate emissions at the point of combustion or emission release based on deterministic
69 information (e.g. fuel combustion characteristics, leak rates) and then aggregate these to an implied
70 national total. The top-down approach uses spatial proxies such as gridded population, nighttime
71 lights, GDP estimates, and other available spatial proxy variables to allocate national total emissions
72 across grid cells in each country. Bottom-up techniques often use a mixture of data such as direct flux
73 monitoring (e.g. powerplant stack monitors), local fuel or utility data, and traffic monitoring.

74 Several global and country-scale spatially explicit GHG inventories have been developed based on
75 either bottom-up or top-down approaches. The JRC EDGAR (Crippa et al., 2020), ODIAC (Oda and
76 Maksyutov, 2011; Oda et al., 2018) are well-established examples of global top-down emission data
77 products but others have been developed (Andres et al., 1996; Andres et al., 2016; Asefi-Najafabady
78 et al., 2014; Nassar et al., 2013; Rayner et al., 2010; Wang et al., 2013), including some at the
79 national/regional scale (Bun et al., 2019; Zheng et al., 2021; Jones et al., 2020; Kurokawa et al., 2013;
80 Meng et al., 2014). A number of these models use nighttime lights data as one input signal (or gridded
81 population datasets which in turn may be based on nighttime lights), though at least one study has
82 found this is only moderately predictive (Gaughan et al., 2019).

83 Spatially-explicit bottom-up GHG inventories have been accomplished at the regional, national and
84 urban scale. For example, the US 1 km²/hourly Vulcan CO₂ emissions data product (Gurney et al.,
85 2020a; Gurney et al., 2009; Gurney et al., 2020b) and the Northeast US 1km² ACES (Gately and Hutyra,
86 2018) data product. Similarly, work in Poland has achieved similar success (Bun et al., 2010; Bun et al.,
87 2019) Building/street scale bottom-up efforts have also been accomplished with the Hestia Project
88 which has estimated hourly urban CO₂ data products in the four US cities (Gurney et al., 2019; Gurney
89 et al., 2012; Patarasuk et al., 2016; Roest et al., 2020).

90 Finally, urban emissions have been estimated at the whole-city scale using both top-down and
91 bottom-up techniques as individual city studies or as collections of urban areas (Ramaswami and
92 Chavez, 2013; Chen et al., 2019; Harris et al., 2020; Jones et al., 2020; Meng et al., 2014; Shan et al.,
93 2018; Shan et al., 2017; Zheng et al., 2021; Long et al., 2021)

94



95

96 as well as results focused on city results in England (Baiocchi et al., 2015), China (Liu et al., 2020; Wang
97 et al., 2017), and Europe (Baur et al., 2015). Many of these studies extend analysis to include Scope 3
98 or consumption emissions.

99 Here we provide a new pan-European emissions inventory at the municipality level (Moran, 2021).
100 This is intended to be useful for cities which have not conducted their own inventory. The inventory
101 disaggregates the totals from the official national CO₂ inventory, summarizing the 167 line items of
102 the IPCC's 2006 Common Reporting Framework (hereafter, CRF) (ipcc, 2006) into 9 emissions
103 categories. The model identifies up to 5 levels of administrative hierarchy (totaling 116,210
104 administrations) across 34 European nations including the UK.

105 This paper proceeds by first situating this contribution with respect to similar work. We then present
106 the methodology and results, including a pixel and city-level comparison with existing models and a
107 first validation against 43 existing urban emissions inventories assembled by individual cities. We
108 conclude with a discussion in which we reflect on use cases and next steps.

109 The JRC EDGAR database, ODIAC, and GCP-GridFED databases are obvious points of comparison to the
110 model we present in this study. Section 3 presents a conceptual and numerical comparison of these
111 models. The main innovations presented by this model over EDGAR and ODIAC are (a) results are
112 provided for administrative jurisdictions rather than on a raster grid and (b) the use of OpenStreetMap
113 is novel. Additionally, our model is targeted to be useful to citizens and policymakers in city and local
114 governments by illuminating where CO₂ emissions in their city arise from. This influences some of our
115 modeling approaches, such as attributing emissions from ships and planes to ports and airports rather
116 than along their physical voyage tracks. But it is the provision of ready-to-use results at the city,
117 county, and state level across Europe which we believe is the core contribution of this database.

118 The method described here is intended for creating an inventory of direct emissions. It is worthwhile
119 to recall the distinction between scope 1, 2, and scope 3 emissions inventories as defined in the WRI's
120 Greenhouse Gas Protocol nomenclature (WRI et al., 2014). An inventory of direct emissions is called a
121 scope 1 inventory, a territorial emissions account, or a production-based emissions account (PBA). A
122 scope 2 inventory will be largely identical to a scope 1 inventory but reallocate the emissions from
123 electricity production to the location where that electricity is directly used. A scope 3 inventory, also
124 called a footprint or a consumption-based account (CBA), will further expand the scope and attribute
125 to consumers all emissions associated with imported goods and services produced domestically or
126 abroad, and emissions associated with waste exported outside the jurisdictional bounds. For urban
127 areas with little production and much consumption, scope 3 emissions can be substantial: studies
128 estimate that for many urban cores their scope 1 emissions are 30-50% of their total scope 3 footprint.
129 Scope 3 inventories are estimated using trade and supply chain databases and rely on robust (i.e. well-
130 modeled or empirically validated) scope 1 inventories as a starting point. There is an active community
131 working to prepare Scope 3 assessments at the city level (Chen et al., 2019b, a; Guan et al., 2020;
132 Heinonen et al., 2020; Minx et al., 2013; Moran et al., 2018; Pichler et al., 2017; Ramaswami et al.,
133 2021; Wiedmann et al., 2021; Zheng et al., 2021b).

134

135 **2. Methods**

136 The approach presented here spatializes the national emissions inventory using activity data from
137 Open Street Map (OSM), the EU's Emissions Trading System registry of point source emitters, and
138 traffic data for airports. This method sums to a national total equal to the national inventory,
139 generates results as both a gridded dataset and per administrative unit and preserves detail on the
140 sources of emissions. The intention is to best locate emissions to where they physically or legally occur.



141 As the spatial resolution of the inventory increases an interesting consideration emerges, namely that
142 there is some discretion in where emissions should be spatially located. The emissions for a passenger
143 ferry for example could be spatially located over water where they physically occur, at the office of
144 the ferry company which is legally responsible, at an industrial harbor where the boat takes on fuel,
145 or at the passenger terminals where it traffics. At larger grid cell sizes these four locations are more
146 likely to share the same grid cell, but with highly resolved models this becomes a modeling choice.
147 Our choices on such decisions are documented in the relevant section of methods which describes
148 each emissions category, but as a general principle we opt to locate emissions where it makes most
149 sense for communication and outreach by those using the results, where policy tools are easiest to
150 apply, or where they physically occur, in that order.

151 Scope of coverage: The model is currently built for the year 2018. This is the most recent year for
152 which official national inventories were available from EUROSTAT when the model was assembled.
153 The list of countries covered is provided in the Results section of this paper. The UK is included in the
154 model. Regarding the impact of the UK's exit from the EU, we anticipate this will not substantially
155 reduce the ability to use this model for the UK, since the UK has established its own UK ETS and, we
156 presume, will continue to publish an emissions inventory in CRF (the IPCC's Common Reporting
157 Format) format. This study focuses only on CO₂ emissions; other greenhouse gasses are not included.
158 In each relevant section of the Methods a discussion is included about how the model could be
159 extended to handle other GHGs. One rationale for this choice is that the second largest GHG, CH₄, is
160 heavily driven by agricultural activities and rogue emissions and these are some of the hardest to
161 accurately spatialize. Furthermore, the intention in this study is to focus on fossil fuel use and not
162 short-cycle carbon such as emissions related to land use and agriculture. Therefore, the model does
163 not include emissions from land use, land-use change, and forestry (LULUCF). The choice to exclude
164 these from the model was based on considerations including (a) estimates of total LULUCF emissions
165 are often poorly constrained, (b) they are difficult to spatialize accurately, (c) local government policy
166 have fewer immediate policy options for managing these emissions, (d) national climate targets often
167 exclude LULUCF emissions, (e) there are diverse approaches to accounting for LULUCF and carbon
168 sinks, leading to significant variability.

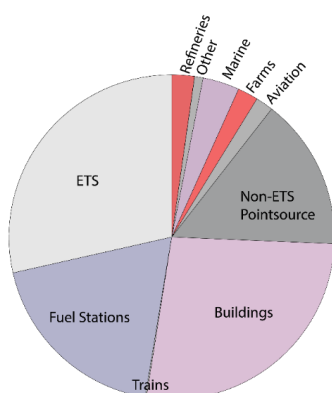
169 The model assembly procedure can be summarized as follows. Further detail and discussion on each
170 aspect is provided in the following subsections. First, emissions which can be attributed to point
171 source facilities reporting under the ETS are separated from the national inventory. ETS-registered
172 emissions are geolocated at the street address registered for that permit holder. In the cases where
173 the location of emissions differs from the registered address (e.g. offshore oil activities, or some
174 company activities) this approach can still be rationalized since (a) physically locating all facilities which
175 are not at their mailing address will be difficult, and (b) legally, the control of the emissions is likely at
176 the registered address, so there is sense in calling attention to emissions which are controlled from
177 there. Emissions from vehicles are apportioned equally to fuel stations as located in OSM. The model
178 amortizes total national vehicle fuel use evenly across all fuel stations, though this will not correctly
179 capture subtleties such as fleet and trucking-only fuel depots, nor differentiate between small (1-2
180 pump) stations and large filling stations with multiple pumps. Emissions which are associated with
181 buildings (heating and cooling, construction, and light commercial activity), plus the residual industrial
182 emissions which cannot be attributed to ETS sources, are apportioned equally onto all buildings
183 registered in OSM. (OSM does allow buildings to be tagged with extended attributes such as floor size,
184 stories, and use, but in our investigations <1% of buildings use these attributes so for now we have
185 not attempted to utilize those fields.) Emissions from marine bunker fuels are apportioned equally to
186 harbors as located in OSM (note that diesel fuel for small vessels will be treated as vehicle fuel).
187 Emissions from aviation bunker fuel are spatialized onto airports proportional to the volume of
188 passenger traffic handled at each airport, as reported by Eurostat. Fugitive emissions and emissions
189 from petroleum byproducts are spatialized equally across national refineries and associated oil
190 storage facilities. CO₂ emissions from farming and forestry are apportioned to farmed areas as located



191 in OSM (these are based on the EU CORINE land use map). Emissions from trains are mapped to
192 passenger train stations.

193 Figure 1 displays the total emissions covered in the model, excluding of LULUCF and carbon sinks,
194 grouped according to the methods used to spatialize those emissions, and color coded according to
195 the approximate level of difficulty, or degree of uncertainty, of that spatialization, with greyer colors
196 representing more easily spatialized emissions and brighter colors indicating emissions categories
197 which, in the authors' experience, are more difficult to confidently spatialize.

198



199

200 *Figure 1: Composition of emissions across the 34 European countries covered. ETS shows the volume of emissions associated*
201 *with ETS-registered point source emitters; fuel stations show emissions from vehicles; the 'buildings' category comprises*
202 *emissions from building heating, cooling, construction, and light commercial activity. Non-ETS point source emissions is a*
203 *residual category representing the difference between industrial emissions as reported in the national inventory and the sum*
204 *of emissions reported by facilities participating in the ETS. Nearly half (42%) of these occurs in Turkey, which as of publication*
205 *does not participate in the ETS, but this discrepancy is also observed in large emitters like Germany, France, the UK, and*
206 *Poland. These residual emissions are spatialized using OSM records instead of ETS addresses.*

207

208 a. Mapping point source emissions regulated by the EU Emissions Trading System

209 The EU's Emission Trading System (ETS) requires large point-source emitters to report emissions and
210 report an address for every permit holder. A geolocation API was used to translate these addresses
211 into latitude-longitude coordinates. While for many facilities the address where the emissions are
212 legally controlled is the same as the facility's physical address, or in a nearby town, in some cases the
213 two locations can differ more substantially (emissions from Norwegian offshore activities are largely
214 legally controlled in the city of Stavanger, for example). The emissions associated with ETS permitted
215 facilities are then subtracted from the CRF inventory thus leaving fewer total emissions remaining to
216 be spatialized. The allocation of CRF emissions to ETS facilities is done as follows. For a number of CRF
217 sectors (for example, "Fuel combustion in manufacture of iron and steel" (1.A.2.A)), some or all of the
218 sector's emissions are attributable to ETS facilities. We constructed a priority-ranked concordance
219 table to determine which CRF emissions are already covered by ETS-registered permits. Normally the
220 ETS-reported emissions for a given activity are less than or equal to the CRF-reported emissions for
221 that category and there is only a small residual between the CRF-reported value and sum across
222 pertinent ETS permits, however in some cases this residual is substantial.

223 The mapping between ETS categories and CRF categories is not always one-to-one. For example, the
224 ETS uses the code "24: Production of pig iron or steel". These facilities may correspond to the CRF
225 activities, Fuel combustion in manufacture of iron and steel (1.A.2.A), Iron and steel production (2.C.1),
226 or Ferroalloys construction (2.C.2). In our ranked concordance matrix approach, a rank of 1 is given to



227 the first CRF activity, a rank of 2 is given to the second CRF activity, and a rank of 3 is given to the third
228 CRF activity. The emissions from those ETS facilities from code 24 are first attributed to the rank 1 CRF
229 activity until it is sated, then excess ETS emissions are assumed to come from the rank 2 activity until
230 that volume is sated, the same for rank 3, and so on. Using the above example that could mean that
231 all emissions under the first two CRF categories would be fully attributed to ETS iron and steel facilities,
232 and a portion of the emissions under rank 3, Ferroalloys construction (2.C.2), which cannot be
233 attributed to ETS facilities, would remain to be spatialized.

234 In some cases it is unclear what the ranking of CRF activities should be. For example after allocating
235 ETS emissions from “production of lime, or calcination of dolomite/magnesite” (ETS category 30) first
236 to lime production (2.A.2) and secondarily to glass production (2.A.3), should excess ETS facility
237 emissions from code 30 best be attributed to Cement production (2.A.1), Fuel combustion in
238 manufacture of non-metallic mineral products (1.A.2.F), or Fuel combustion in other manufacturing
239 industries and construction (1.A.2.G)? In this case the last three sectors are sated in smallest-to-largest
240 order until no ETS emissions remain to be allocated. The rationale for the ascending sort order is that
241 larger CRF categories will be easier to spatialize using other methods. In the earlier example of
242 aluminum production, any surplus reported in ETS which exceeds the CRF reported aluminum
243 production emissions is then assigned to the rank 2 CRF category of “Fuel combustion in other
244 manufacturing industries and construction”, decreasing the amount of emissions in that CRF category
245 which remain to be spatialized. We also note that not all facilities use the expected ETS activity code.
246 For example we have observed some fertilizer plants reporting emissions under ETS activity code 42
247 “Other Bulk Chemicals” instead of activity 41, “Ammonia production”. Such misattributions can
248 introduce distortions in the model results. To characterize the impact of these distortions the
249 allocation of ETS emissions through the ranked priority allocation system into CRF would need to be
250 followed manually in detail.

251 After linking ETS-reported emissions to the national inventory, the remaining CRF-reported emissions
252 are spatialized using the methods described as follows.

253

254 **b. Vehicles**

255 These are emissions from the following five CRF categories

- 256 1.A.3.B.i Fuel combustion in cars
- 257 1.A.3.B.ii Fuel combustion in light duty trucks
- 258 1.A.3.B.iii Fuel combustion in heavy duty trucks and buses
- 259 1.A.3.B.iv Fuel combustion in motorcycles
- 260 1.A.5.B Mobile fuel combustion sectors n.e.c.

261 These emissions are specialized according to the location of vehicle fueling stations as documented in
262 OpenStreetMap. We make the assumption that the number of vehicle fuel stations in an area is
263 proportional to the volume of traffic served. This is a simplifying assumption and it is clearly
264 communicated in the model presentation. In future development of the model, localizing vehicle
265 emissions will be a top priority. This approach assumes that every fuel station supplies a similar level
266 of vehicle traffic. It could be the case that some stations are small single pump gas stations while
267 others are large facilities, for example such as located along a major highway rest stop. To address this
268 one future solution could be introduce better road traffic estimates. While traffic load estimates are
269 available for some roads, these estimates tend to be for only a few dozen specific highways. Fu and
270 colleagues (Fu et al., 2017) proposed a method using neural networks to estimate vehicle flow on
271 every road using OSM data and gridded population models. (Osses et al., 2021) recently prepared a
272 high-resolution map of emissions from vehicles in Chile. Better modeling vehicle traffic, not only fuel
273 station availability, would make the model more accurate in spatially estimating vehicle fuel
274 emissions. Another potential solution would be to identify data on fuel station volume, e.g. sales



275 estimates or number of pumps installed, but this may be challenging in practice. A second assumption
276 is that every station serves a homogeneous mix of vehicles. It may be the case that some stations
277 serve a specific fleet, for example a city bus fleet, and better identifying the mix of vehicles served by
278 each fuel station would allow the above five emissions categories to be more precisely spatialized.
279 Insofar as electric car adoption drives some fuel stations to close the model will reflect lower vehicular
280 emissions in areas with more electric vehicles. An interesting note is that in some urban centers light
281 truck traffic is suspected to be a larger emission source than passenger vehicles. Better distinguishing
282 types of traffic and vehicles would be useful for helping guide decarbonization plans that are most
283 appropriate for various areas.

284

285 **c. Trains**

286 Trains are a relatively minor source. Emissions for Fuel combustion in railways (1.A.3.C) were
287 spatialized using passenger train stations as reported in OSM. Every train station was allocated an
288 equal share of the total emissions. A limitation of this approach is that it may be that not all train
289 traffic is equally fuel-intensive: some individual trains or sections of the rail network could be fully
290 electrified and other areas not. Another limitation is that the method allocates total train emissions
291 (both passenger and cargo) equally across passenger stations, yet passenger stations are not all
292 equally used, and cargo train activity would be more appropriately localized at freight yards. Reporting
293 train emissions at passenger terminals does service a communicative value as it reminds viewers that
294 train traffic is not entirely emissions-free.

295

296 **d. Buildings**

297 In the following categories, only a portion of the emissions can be spatialized to ETS locations, but
298 there remain emissions which must be spatialized onto buildings:

- 299 1.A.2.G Fuel combustion in other manufacturing industries and construction
- 300 1.A.4.A Fuel combustion in commercial and institutional sector
- 301 1.A.4.B Fuel combustion by households
- 302 1.D.3 Biomass - CO₂ emissions (memo item)
- 303 2.D.3 Other non-energy product use

304 The largest shares of these remaining emissions are driven by building heating and cooling and fuel
305 combustion by light industry and construction.

306 Correctly spatializing these emissions associated with buildings is a substantial challenge. OSM is
307 sometimes known as Open Buildings Map since the database actually contains more buildings than
308 streets. The OSM dataset reports an extensive number of buildings, but little data is available to
309 characterize each building. OSM does not record all buildings. In many areas, including small towns,
310 only a street address is marked but there is no point or polygon data indicating what is built at that
311 address. While it might be possible to obtain maps of all buildings from national cadaster agencies,
312 part of our intention in the model is to develop methods which are replicable across other countries
313 and not rely on single-country datasets. Of the buildings recorded in OSM, only a small percentage (1-
314 5%, depending on country) contain any information characterizing the building such as number of
315 floors, main usage activity, building material type, or building age. Some recent offerings which
316 provide building footprints (e.g. products from Maxar or Predicio Building Footprint Data, free
317 offerings from Bing / Microsoft, and academic initiatives such as coordinated through spacenet.ai)
318 could be used to identify at least building footprint size, and potentially height or construction
319 material.

320 The approach used in the model is to apportion all of the emissions associated with buildings equally
321 among all buildings and registered street addresses in each country. It is important to recall that for



322 buildings heated by electricity, CO₂ emissions associated with electricity production will be located at
323 ETS-registered power plants. As noted above, there is a paucity of information available by which we
324 could further characterize building size or use.

325

326 e. Aviation

327 Total emissions associated with kerosene used for aviation fuel (the sum of CRF emissions categories
328 “Fuel combustion in domestic aviation (1.A.3.A)” and “International aviation (1.D.1.A)”) are attributed
329 to airports proportionally to total passenger kilometers (pkm).

330 Total pkm are derived from the combination of EUROSTAT statistics of route traffic and passenger
331 traffic per airport. This procedure is preferred over an attribution based solely on total passenger or
332 flight numbers, since we here implicitly incorporate information on both the flight length and aircraft
333 size. These parameters are two major drivers for fuel consumption and emissions (Yanto and Liem,
334 2018).

335

336 f. Farming Activity

337 The CRF uses the following three categories for farming-associated activities:

- 338 1.A.4.C Fuel combustion in agriculture, forestry and fishing
- 339 3.G Liming
- 340 3.H Urea application

341 The largest of these, category 1.A.4.C, is challenging to spatialize for two reasons: First, the inclusion
342 of fishing activity means emissions in this category overlap with emissions in marine traffic. To handle
343 this, emissions from fishing would have to be estimated, removed from this amount, and spatialized
344 separately. Even then, the remaining emissions from fuel combustion in agriculture and forestry would
345 still be difficult to spatialize. Second, we have not been able to identify a suitable dataset to use to
346 divide and appropriately spatialize forestry as distinct from farming.

347 Our approach is to map these collected emissions onto locations of farmland as identified by the EU’s
348 CORINE land-use dataset, which is already incorporated into OSM. The above emissions were evenly
349 allocated to the centroid points of all polygons tagged as farmland from CORINE. This approach will
350 not correctly spatialize emissions associated with forestry. Also, this approach allocates the emissions
351 evenly across every polygon tagged as farmland, regardless of the size of each patch. A future
352 improvement could be to weight this allocation by patch size and thus assume every hectare of
353 farmland is equally emissions-intensive to manage, or to introduce activity-level data for agriculture,
354 such as integrating maps of dairy cattle operations (Neumann et al., 2009) or similar.

355 As discussed in the introduction, and in section 10 below on short-cycle carbon, currently the model
356 intentionally excludes emissions from land use, land use change, and biotic processes such as cattle
357 digestion and manure handling.

358 The following categories in the CRF report also relate to farming:

- 359 3 Agriculture
- 360 3.1 Livestock
- 361 3.A Enteric fermentation
- 362 3.B Manure management
- 363 3.C Rice cultivation
- 364 3.D Managed agricultural soils
- 365 3.E Prescribed burning of savannas
- 366 3.F Field burning of agricultural residues



367

368 **g. Marine**

369 Emissions in this sector are comprised of the following CRF emissions categories:

370 1.A.3.D 4 Fuel combustion in domestic navigation

371 1.D.1.B 4 International navigation

372 This covers tank-to-wake emissions that stem from fuel combustion. Total fuel consumption is
373 calculated by a top-down assessment based on annual sales of bunker fuel in each country, comprising
374 marine gas oil (MGO) and heavy fuel oils and distillates (HFO), and geospatially distributed across the
375 888 ports.

376 Port-allocation of bunkered fuels is based on the total transport work for berth-to-berth ship voyages,
377 as obtained from IHS Markit, totaling 773 000 port calls. Ship voyages are combined with their ship's
378 respective average fuel consumption as reported by shipowners to the European Union's emissions
379 monitoring scheme (the EU MRV, Monitoring, Reporting and Verification), given as kilograms of fuel
380 per nautical mile. This covers all vessels operating in EU ports above 5000 GT, totalling approximately
381 11 000 vessels. The distance covered with each voyage is calculated by applying the Dijkstra's
382 algorithm (Dijkstra, 1959) to find the shortest path between two ports, followed by a curve smoothing
383 process by the Ramer–Douglas–Peucker algorithm (Douglas and Peucker, 1973; Ramer, 1972). The
384 average fuel consumption and distance sailed is used to estimate total bunker demand at the port
385 level, by weighing the national reported bunker sales.

386 This assessment does not include leisure crafts, considered negligible in comparison to cargo vessels,
387 neither does include warships, naval auxiliaries, fish-catching or fish-processing ships that are exempt
388 of reporting their activity to MRV.

389

390

391 **h. Other**

392 There are some emissions which are difficult to spatialize. These are:

393 1.C Transport and storage of CO₂ (memo item)

394 2.A.4 Other process uses of carbonates

395 2.D.1 Lubricant use

396 2.D.2 Paraffin wax use

397 In the model these emissions are included in and spatialized using the same strategy as emission from
398 buildings as described above.

399

400 **i. Refineries**

401 The following CRF emissions categories are associated with oil refineries and fossil fuel infrastructure:

402 1.B 2 Fuels - fugitive emissions

403 1.B.1 Solid fuels - fugitive emissions

404 1.B.2 Oil, natural gas and other energy production - fugitive emissions

405 2.B.8 Petrochemical and carbon black production

406 Carbon black, item 2.B.8, used to produce black ink, is a byproduct from fracking at refineries. Fugitive
407 emissions (1.B.2) are by their nature difficult to spatialize (Plant et al., 2019). A number of studies in
408 California have tried to characterize fugitive emissions from the ageing oil wells and modern fracking
409 equipment in the region (Hsu et al., 2010; Rafiq et al., 2020; Townsend-Small et al., 2012; Wennberg
410 et al., 2012). In our model all fugitive emissions are attributed evenly across refineries and associated



411 storage tanks as located in OSM. The fugitive emissions are apportioned equally among the buildings
 412 tagged [industrial=refinery] or [industrial=oil] in OSM. This approach has the disadvantage of not
 413 correctly spatializing fugitive emissions at the various wellheads, pumping and storage locations
 414 where such emissions physically occur, but has the advantage of attributing fugitive emissions to
 415 refineries so that policy planning can recognize that fossil fuel creates emissions both when it is
 416 combusted but also during its production. This approach follows the guiding philosophy of locating
 417 emissions where they best connect to the relevant policy discussion.

418

419 **j. Short-cycle carbon (Land Use, Forestry, and Stock Change)**

420 Our model is focused on reporting CO₂ emissions from fossil fuel combustion and industrial processes.
 421 Carbon put into sinks (under CRF section 5 - Waste), either natural (terrestrial, aquatic, or marine) or
 422 manmade (e.g. timber construction or paper or biomass put into landfill) sinks is not spatialized or
 423 included in the results. Negative emissions from carbon capture and storage facilities are presently
 424 excluded from the model.

425 CO₂ emissions from CRF category 4, encompassing land use, land use change, and forestry, are also
 426 not included. Our intention is to spatialize fossil fuel combustion associated with agriculture and
 427 forestry but not emissions associate with landscape-scale soil and biotic processes. We reason that
 428 such landscape-scale emissions are both large, and very challenging to address using locally available
 429 policy tools. Including them in a city-oriented plan, particularly in rural municipalities, could lead to a
 430 situation where the results are heavily dominated by an emissions category with few viable solutions.

431 In future iterations of the model it may be preferable to allow users to easily include or exclude the
 432 emissions in the model results. Currently our model does not include direct CH₄ emissions from cattle
 433 digestion and manure fermentation. This is a substantial emissions category with some remediation
 434 options so it may be useful to include this in a future iteration of the model.

435 Another detail in this category is sewage treatment and landfills. These act as both sources and sinks
 436 of carbon. It is unclear whether net emissions from sewage plants and landfills are included inside the
 437 CRF category “Long-term storage of carbon in waste disposal sites” (5.F.1) or included in another
 438 category. As category 5.F.1 is not included in the model, if net emissions from sewage are included in
 439 this category those emissions will not be included in the model. Quantifying emissions associated with
 440 sewage treatment and local landfills would be an improvement to the model.

441

442 **3. Benchmarking**

443 We do not intend here to provide an exhaustive survey of available spatial emissions models. Here we
 444 only compare the ESCI model with some widely used global-level models. A full comparison of spatial
 445 emissions models, including several strong single-country models, would be a valuable contribution
 446 to the field, but is not within the scope of the present paper. For one such comparison we refer to
 447 (Hutchins et al., 2017).

448 Table 1 provides an overview and comparison of ESCI with ODIAC (Oda and Maksyutov, 2011), JRC’s
 449 EDGAR (Crippa et al., 2019), and the Global Carbon Project’s GCP-GridFED (Jones et al., 2020) spatial
 450 emissions models.

451

	Resolution	Itemization	Temporal	Results by jurisdiction	Scope	Method synopsis
ODIAC	1km	Total emissions	Monthly	Country	Global	Spatialize national emissions using nighttime lights and power plant locations



EDGAR v6.0	0.1° (11km at the equator)	31 IPCC CRF categories	Up to hourly	Country	Global	Collected activity-level data sources (e.g steel industry, FAO for farming activity, ship and flight tracks)
GCP-GridFED	0.1° (11km at the equator)	Total emissions, per 5 fossil fuels	Monthly	Country	Global	National totals from GCP, spatialized using EDGAR
ESCI (our model)	Point-source, 1km grid, or per municipality	9 categories	Annual	Country, State, County, Municipality, facility	Europe	Spatialize national emissions using activity data from OpenStreetMap

452 *Table 1: Comparative overview of several spatial emissions datasets.*

453 Comparison to EDGAR, and GCP-GridFED which uses EDGAR’s spatialization layer: At the time of
 454 writing, the report with the methodology used for the EDGARv6.0 has not been published. Based on
 455 the data sources mentioned at the EDGAR website it appears that activity-level data has been
 456 obtained for various industrial activities (e.g. farming, fertilizer production, steel refineries, electricity
 457 generation), and plane and ship emissions are mapped to voyage tracks, but it is not published how
 458 emissions from buildings, light commercial activity, and vehicles are spatialized, except the GHS-POP
 459 gridded population dataset is mentioned. Since ESCI uses ETS facility-level data to map industrial
 460 emissions (an advantage afforded by its Europe-only focus) it may be that the two models will come
 461 to similar results for mapping industrial emissions since presumably the activity-level datasets for
 462 industry used by EDGAR will be largely identical to the facility-level data from ETS. If EDGAR uses
 463 population density as a proxy to map vehicle and building emissions, this is a slightly different
 464 approach than ESCI’s use of fuel stations and building locations from OSM.

465 Compared to ODIAC: The original ODIAC was a ground-breaking project and introduced the approach
 466 of using power plant locations and nighttime lights as a proxy for emission activities. Since that project,
 467 more recent projects have introduced more proxy variables and activity inventories. In our results
 468 comparison (below) the ODIAC results still agree, but ODIAC does not present results with
 469 sector/activity detail which is important for further insight and to guide action.

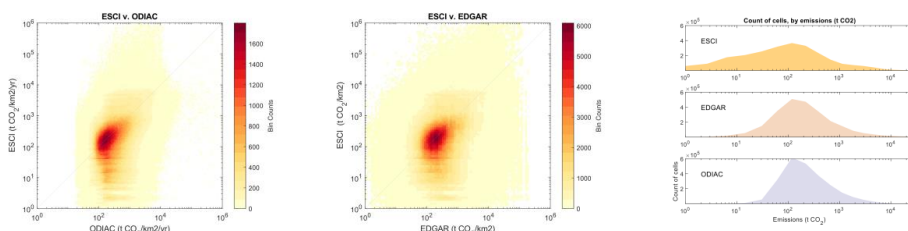
470 In addition to this conceptual comparison of methods we also compare the numerical results. To
 471 compare the results of the ESCI model to ODIAC and EDGAR v6.0 the ESCI model was rasterized to a
 472 30" (arcsecond) raster (approximately 650 m² cells at 45° latitude) to permit a direct cell-level
 473 comparison across emissions models and the GHS-POP gridded population model. The EDGAR dataset
 474 version is v6.0, data year 2018, with a native resolution of 0.1° (360") before re-gridding. For ODIAC
 475 the model version is 2020, with data for 2018, with a native resolution of 1km² cells. The three models
 476 report slightly different totals for total European emissions. This is due (a) to differences in emissions
 477 categories covered, (b) for ODIAC, the monthly allocation, and (c), for EDGAR, the fact that in EDGAR
 478 aviation and marine emissions are spatialized over ship and flight traffic routes rather than allocated
 479 to grid cells in the country. For this initial cross-model comparison, the three datasets were normalized
 480 to include only grid cells covered by all three models and then by normalizing the total emissions
 481 across the three models so that we compare solely the spatial allocation. This is a simplified method
 482 for cross-model comparison and leaves considerable scope for future work on cross-model
 483 comparison. Our main aim here is to document this new model and conduct a preliminary validation,
 484 not conduct a robust cross-model comparison.

485 The cross-model cell-level comparison (Figure 2) shows the degree of convergence between the ESCI
 486 and the EDGAR model. The ESCI reports more cells with low (<100 t CO₂) and very high (>1000t)
 487 emissions. The ESCI model also reports higher cell-level variability than does ODIAC: the ODIAC model
 488 reports most cells have emissions in the range of 10²-10⁴, whereas the ESCI model reports cells with a
 489 range of 10¹-10⁵ t CO₂/yr. This could potentially be an artefact due to aggregation of ODIAC. The ODIAC



490 model is natively provided at 1km² resolution, corresponding to a cell size of 0.07-0.04" depending on
 491 latitude, and it could be that the aggregation to 30" cells for the purpose of comparison has masked
 492 higher variability within the 30" grid. Another hypothesis is that this homogeneity is due to ODIAC's
 493 use of nighttime lights data, and that while illumination is relatively homogenous across urban and
 494 peri-urban areas, the emissions within similarly lit areas can be starkly different. Another noteworthy
 495 feature is that ESCI reports many more areas with low (<100t) emissions compared to both EDGAR
 496 and ODIAC. One hypothesis is that this is related to the method of spatializing emissions from vehicle
 497 fuels to fuel stations. Since fuel stations often are spaced >650m apart, especially in rural areas, this
 498 could result in many pixels in rural areas being assigned zero fuel emissions. As discussed elsewhere,
 499 the decision to localize vehicle emissions at fuel stations was a deliberate design choice in this model.
 500 Other models may choose to localize these emissions on roads, or pro-rate them across a gridded
 501 population map on a per-capita basis.

502

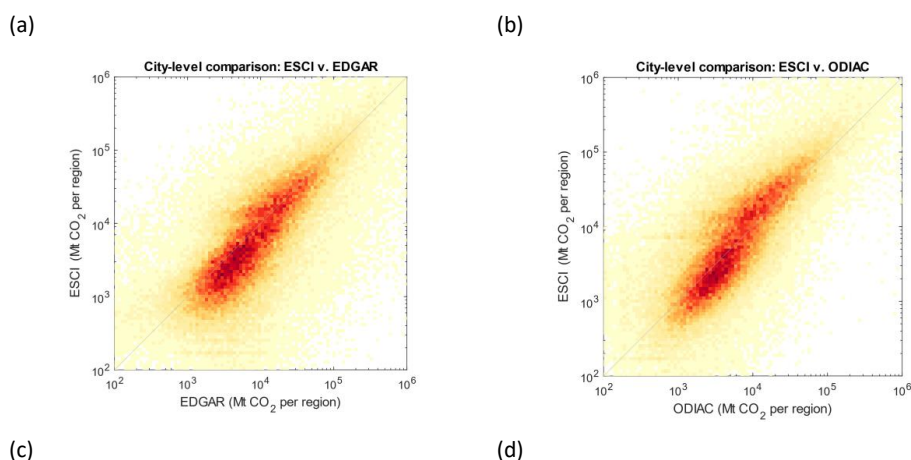


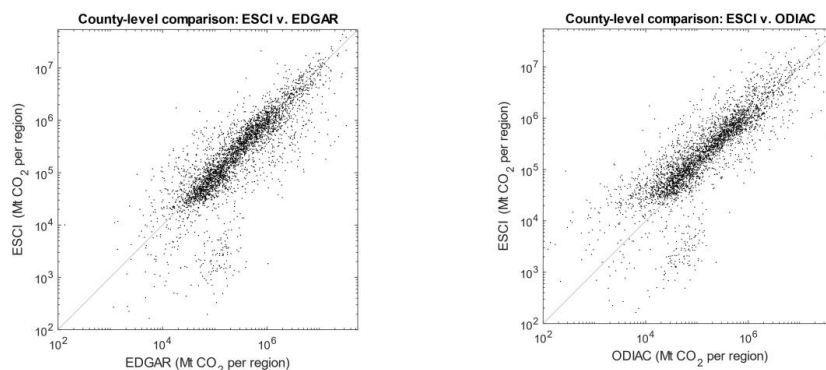
503 *Figure 2: Emissions per standardized grid cell, cross-model comparisons, and frequency analysis. Compared to the ODIAC*
 504 *model (panel a, c), ESCI reports higher cell-level variability, with ODIAC reporting most cells to have emissions in of 10²-10⁴ t*
 505 *CO₂/yr and ESCI reporting cells ranging from 10² to 10⁵ t. Compared to the JRC EDGAR v6.0 model (panel b, c), the ESCI model*
 506 *reports more cells with small (<10² t CO₂) emissions and fewer cells with high (>10⁴ t CO₂) emissions. The ESCI model reveals*
 507 *a higher variability in emissions per cell than do other models.*

508

509 Next, we converted the administrative region definitions from ESCI to a raster map compatible with
 510 the EDGAR and ODIAC gridded datasets. Then we compared the results aggregated by administrative
 511 level (ie. by city) across the models. We compared results both at the city level, i.e. at the highest level
 512 of regional detail per country, and at the county level, i.e. the administrative level one step above that.
 513 These results are presented in Figure 3.

514





515

516 Figure 3: Cross-model comparison of CO₂ emissions per city (using the finest level of regional detail)
517 and per county (using the next-finest level of regional detail per country).

518

519 Currently no methodology has been developed to quantify uncertainty in the model. In addition to
520 being technically challenging, it is difficult to quantify uncertainty in any single portion of the model,
521 much less the whole. Even if the national inventory or ETS inventory are taken to be 100% reliable,
522 errors and biases introduced during the various steps of spatializing these emissions are difficult to
523 quantify. Developing a strategy for parameterizing reliability of model results would be a valuable next
524 step in the research. Previous studies which have investigated techniques for parameterizing
525 uncertainty in gridded spatial proxy models could be useful (Andres et al., 2016; Bun et al., 2010;
526 Hogue et al., 2016; Hutchins et al., 2017; Woodard et al., 2014).

527

528 Validation against city inventories

529 The main objective of the ESCI database is to provide easily accessible estimates for GHG emission
530 inventories at the municipal level to assist local governments in developing more detailed inventories
531 or in developing their own climate action plans (CAP). We compare our ESCI estimates for external
532 validation with existing municipal GHG inventories compiled from a variety of sources in the 343 Cities
533 dataset (Nangini et al., 2019). These emissions inventories are largely self-reported, of varying quality,
534 and follow different protocols, but still provide the most concrete point of comparison for our Scope
535 1 emissions estimates at the municipal level. In total, Scope 1 emission values for 44 European cities
536 can be found in the database, which are compared to the ESCI estimates in Figure 4.

537

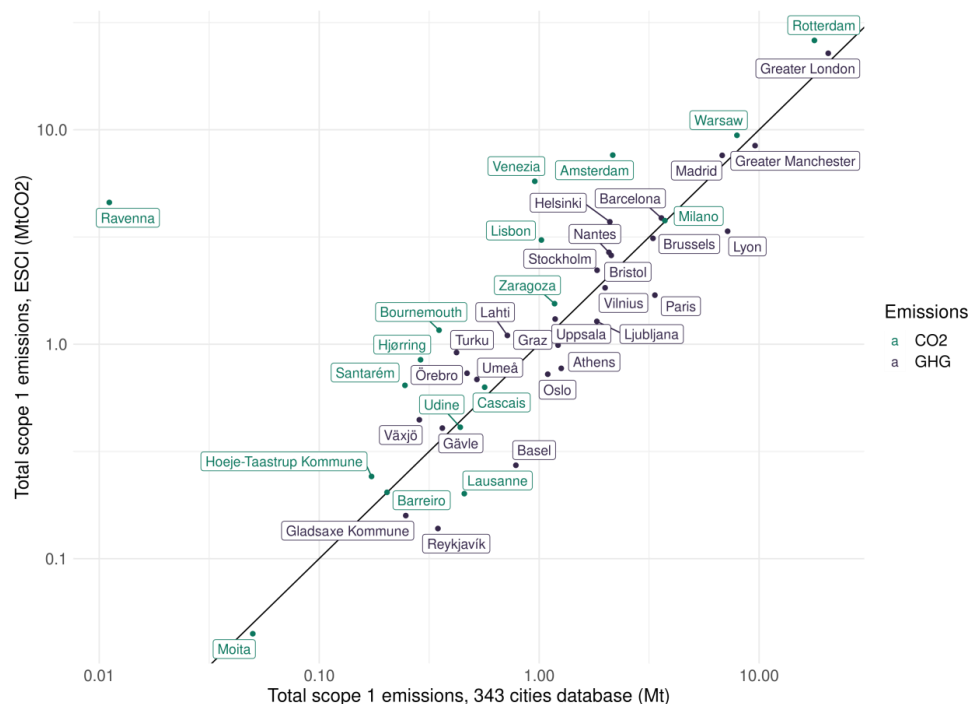


Figure 4: Comparison between ESCI results and the community level emissions inventories of 44 European cities. The color coding indicates whether cities report CO₂ values, or include other greenhouse gases in their inventories.

538

539 The figure shows very high agreement (Pearson correlation coefficient 0.937), despite the different
 540 methods and timing of the city inventories (emission years between 1994 and 2016 with a median of
 541 2013). Only Ravenna, Italy, differs by several orders of magnitude, but the value in the 343-city
 542 database is not realistic (11ktCO₂ for a population of 150000).

543

544 4. Main Findings

545

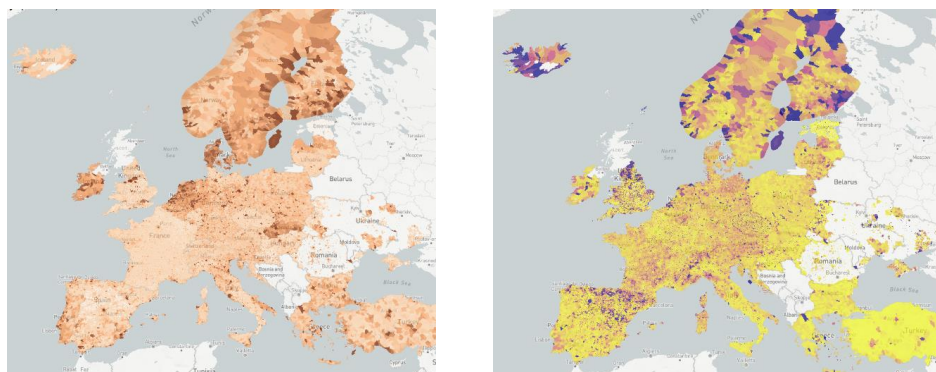
546 a. Results overview

547 An overview of the results for Europe is shown in Figure 5. The results are presented both in absolute
 548 and per capita terms. Some noteworthy features are the high emissions in coastal Netherlands,
 549 associated with marine activity, and the high emissions in Gotland island in the Baltic sea, driven
 550 by one large cement facility there. Emissions in France are remarkably concentrated into a few,
 551 primarily coastal, cities.

552 One limitation which must be kept in mind when looking at the results at the municipal level is that
 553 municipalities vary in size between countries. In continental Europe municipalities are quite small
 554 while in the Scandinavian countries the most local administrative units are relatively large and thus
 555 aggregate more emissions and are more visually prominent. For some analyses, gridded maps, where
 556 the spatial unit of analysis is consistent, are preferable to political maps.

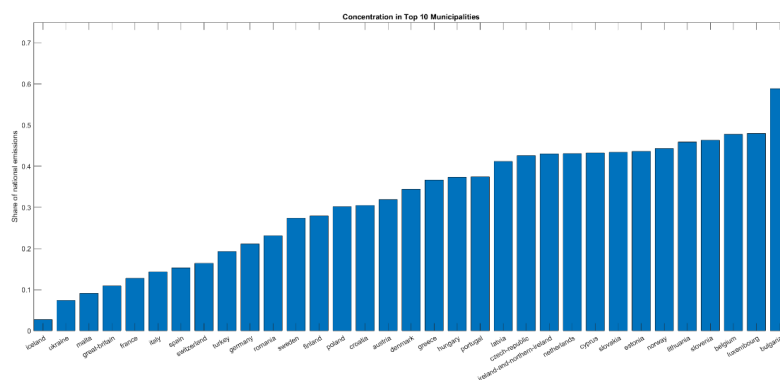


557 Population per administrative area was estimated by overlaying the administrative boundary on the
558 GHS-POP gridded population map. Gray areas indicate areas where no model results are available. In
559 some cases (as seen for example in Ukraine and Romania) the administrative regions at that level are
560 not exhaustive.



561
562 Figure 5: Emissions per municipality in absolute terms (left panel) and per capita terms (right panel).

563
564 In many countries, emissions are remarkably concentrated in a few regions. As seen in Figure 6, in 21
565 of the 34 countries assessed, >30% of national emissions arise from ten municipalities. This implies
566 that focused changes in a few political regions could contribute substantially to achieving national
567 reduction targets.

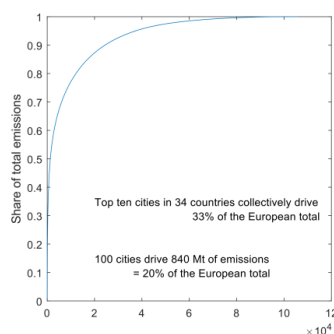


568
569 Figure 6: share of national emissions arising from the top 10 emitting municipalities (or smallest finest
570 administrative distinct) in each country. (Liechtenstein is not shown because the country only has 11
571 municipalities.)

572
573 The important role of high-emitting municipalities is seen at the European level as well. Figure 7
574 presents a Lorenz curve showing the contribution of municipality to the total European emissions. A
575 striking degree of concentration is visible, with 10 municipal regions across Europe driving 7.5% of
576 emissions, 100 driving 20%, and the top 10 cities in each country collectively driving 33.4% of total
577 European emissions. These highest-emitting regions are not necessarily the most populous, since in
578 many cases outlying industrial facilities are major drivers of emissions.



579



580

581 Figure 7: Lorenz curve showing cumulative contribution to total emissions from each municipality.

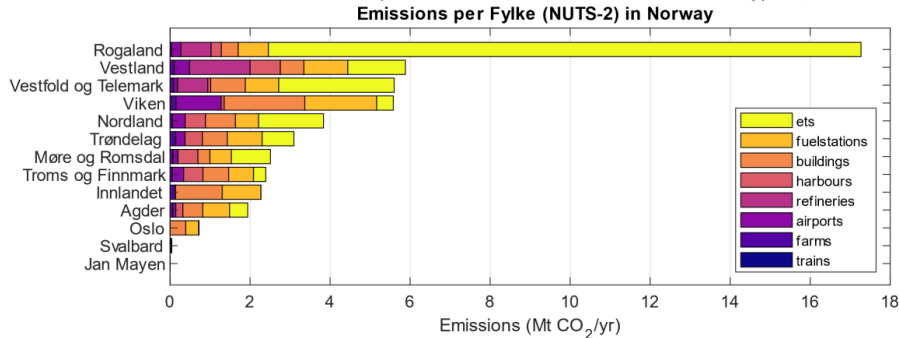
582

583

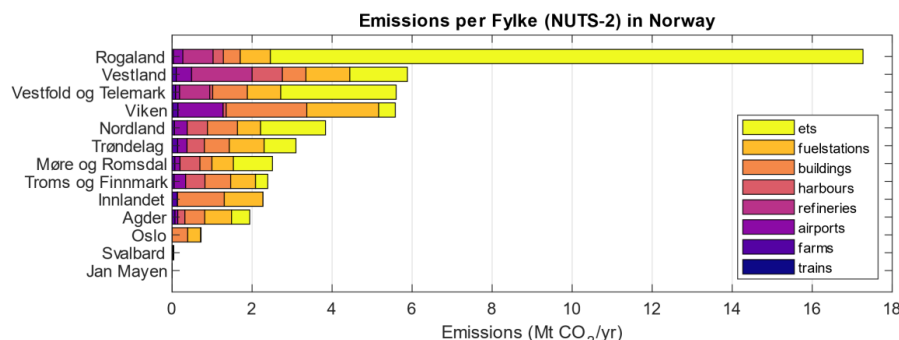
584 **b. Case study of Norway**

585 To demonstrate the results provided by the model we investigate Norway as a case study. In Norway
 586 there are just two levels of administrative hierarchy: counties (*fylke*) and municipalities (*kommune*),
 587 corresponding to the NUTS-2 and NUTS-3 levels respectively. This is a relatively simple configuration;
 588 for many European countries the System of administrative hierarchy is complex and deeply historical.
 589 For example in Germany some cities are peers with states and the administrative configuration is
 590 slightly different between states (in some states there is a level 7 administrative subdivision while
 591 in other states there is not); In Switzerland not all cantons use subdivisions; and in some places statistic
 592 agglomerations of areas, such as capital cities with their suburbs, maybe more relevant than the
 593 judicial regions. Our model provides results at all administrative levels in a country as defined in OSM.
 594 There are up to 10 levels available (we do not include level 11, which is for neighborhoods and
 595 parishes) and most countries use between 2 and 5 levels.

596 The results for Norway at the NUTS-2 (*fylke*) level, (

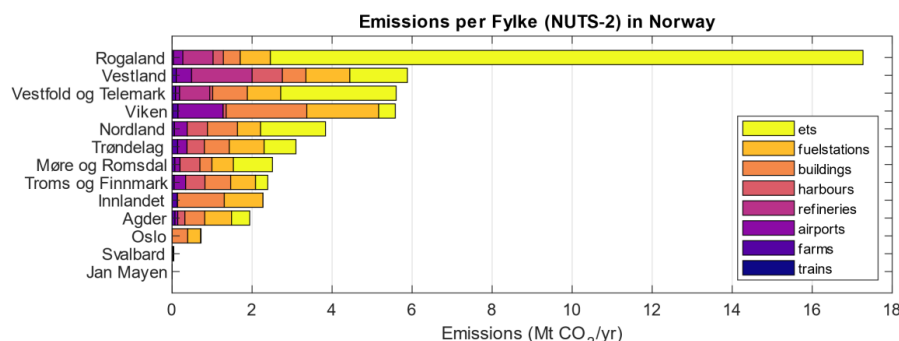


597



598
 599 Figure 8) level show concentration and highlight the importance of industrial sources in Norway.

600 Rogaland fylke is the highest emitting. This is because in Stavanger, a city in Rogaland known as ‘the
 601 oil capital of Norway’, in addition to reported emissions from petroleum facilities physically around
 602 the city, many of the ETS-registered point source emissions from offshore facilities are legally
 603 registered to company offices in Stavanger.



604
 605 Figure 8: Emissions per NUTS-2 region (fylke) in Norway. The very high emissions in Stavanger (Rogaland) are driven largely
 606 by ETS-registered point sources. Stavanger is known as the oil capital of Norway. Note that Oslo fylke itself is small (ranked
 607 11th), coextensive with only the heart of the city, and that Viken (ranked 4th) is the region which encompasses the greater Oslo
 608 region.

609 Viken, the region of greater Oslo, has 5.8Mt of CO₂ emissions. The model results show that 32% of
 610 these emissions come from vehicles and 36% from buildings. Fossil fuel heating has been phased out
 611 of most buildings in Norway so these emissions are from light commercial activity, such as small
 612 burners, boilers, and generators not reporting to the ETS. A full 20% of emissions in Viken (1.1Mt) are
 613 associated with Norway’s largest airport, the Oslo airport at Gardermoen. As described in the
 614 Methods, total emissions from aviation bunker fuel use in the country are allocated across airports in
 615 the country pro-rated by 2018 passenger volume. This approach could be biased and emissions from
 616 cargo flights, long-haul flights, and military aviation, should be located at airports different from those
 617 handling the most passenger traffic. This is a limitation of the current model.

618 Table 2 presents results at the municipality (*kommune*, or LAU-1) level for the top 20 municipalities.
 619 The relatively low emissions from the cities of Oslo (ranked 11th), Bergen (ranked 10th) and
 620 Trondheim (ranked 19th) is surprising given these are the three largest cities in Norway. Industrial
 621 emissions from ETS sources are the primary emissions drivers for the top four cities. The city-level
 622 results do also reveal some challenges with the model. The “refineries” category is defined as the
 623 residual between the national total emissions associated with industrial facilities and the total
 624 reported by the ETS facilities, and this residual is allocated evenly across facilities tagged as “refineries”
 625 in OSM. Overall this residual is small, but since there are few refineries, for individual cities it is
 626 substantial. Also noteworthy are the major emissions from harbors in the residential island

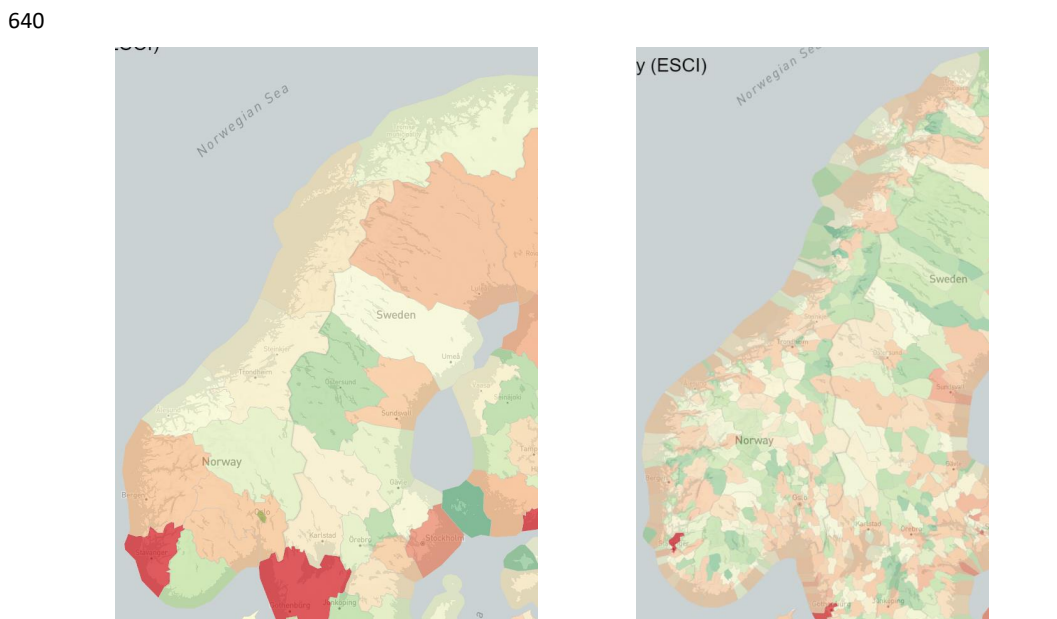


627 archipelago of Øygarden. Currently emissions from marine bunker fuel are allocated evenly across all
 628 facilities tagged as “harbor” in OSM. In Øygarden there are many small-boat facilities, often not even
 629 selling fuel, yet at the same time the island region outside of Bergen is also heavily trafficked by large
 630 offshore work ships and cargo ships. Improving the methods use for spatializing emissions from
 631 marine bunker fuel use would help improve the model for Norway and other countries with extensive
 632 marine traffic.

Municipality (kommune)	Total	Airports	Buildings	ETS	Farms	Vehicles	Harbours	Refineries	Trains	TiOx
Stavanger	12,109,439	-	149,270	11,779,396	4,935	146,650	28,932	-	256	-
Porsgrunn	2,079,447	-	17,446	1,989,186	441	67,040	4,822	-	512	-
Sola	1,395,161	208,654	23,320	1,100,663	448	37,710	24,110	-	256	-
Tønsberg	1,262,066	-	81,972	347,759	3,731	67,040	4,822	756,230	512	-
Ullensaker	1,223,520	1,128,279	29,898	-	1,981	62,850	-	-	512	-
Haugesund	1,202,557	-	17,292	1,133,338	1,015	46,090	4,822	-	-	-
Øygarden	1,088,329	-	37,224	67,910	2,695	79,610	144,660	756,230	-	-
Sandnes	905,490	-	56,100	-	980	92,180	-	756,230	-	-
Alver	864,906	-	31,174	-	9,198	58,660	9,644	756,230	-	-
Bergen	729,745	331,913	157,344	30,033	3,353	205,310	-	-	1,792	-
Oslo	724,800	-	386,628	10,468	2,002	322,630	-	-	3,072	-
Sunddal	694,376	-	8,008	670,648	3,150	12,570	-	-	-	-
Karmøy	616,538	27,177	20,218	442,562	413	58,660	67,508	-	-	-
Bamble	596,183	-	3,388	541,806	77	46,090	4,822	-	-	-
Rana	584,501	20,400	7,920	503,573	6,006	46,090	-	-	512	-
Vefsn	530,372	14,620	34,936	446,234	294	33,520	-	-	768	-
Fredrikstad	518,362	-	186,010	71,105	8,722	117,320	9,644	-	256	125,305
Årdal	467,475	-	2,288	456,373	434	8,380	-	-	-	-
Trondheim	458,851	-	233,640	45,422	2,289	167,600	9,644	-	256	-
Senja	451,891	-	27,962	304,611	266	41,900	77,152	-	-	-

633
 634 Table 2: Estimated emissions for 2018 for the top 20 emitting municipalities in Norway, as generated by ESCI.

635
 636 The model can be explored as tabular data, as a gridded raster model, or visualized on a map. Figure
 637 9 provides an overview of the distribution of emissions across Norway, aggregated at the county and
 638 municipality levels. A concentration of emissions in Stavanger (in the southwest corner) and Porsgrunn
 639 (an industrial area in the south) is clearly visible.

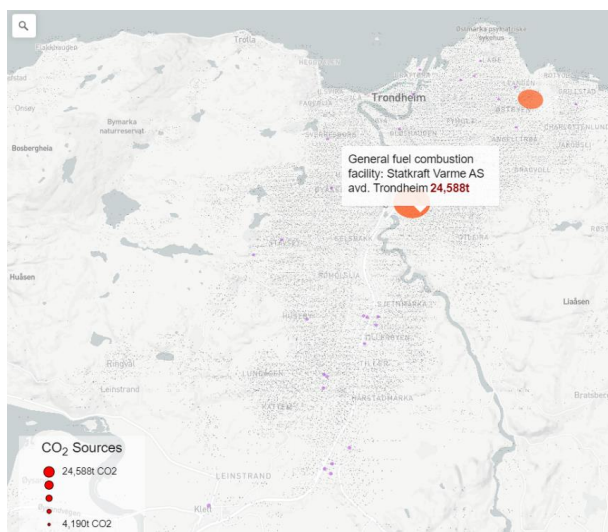


641 Figure 9: Heatmap visualization of ESCI-estimated emissions at the NUTS-2 county level (left) and municipality level (right) in
 642 Norway. Regions are color coded from green (lowest) to red (highest) emitting region in the country.



643 Internally, the model attributes all national emissions to points across the country. It is possible to
644 zoom in and view these emission point sources. Figure 10 provides a screenshot from the model
645 visualization for the city of Trondheim, a city of 200,000 located in mid-Norway. The dots over each
646 building, farm, fuel station, and ETS facility are scaled according to the estimated amount emissions
647 coming from that point. Orange dots show ETS-registered facilities. Purple dots in the figure show fuel
648 stations. The fine grey dots in the figure show all buildings registered in OSM. As detailed in the
649 Methods, emissions from several categories are allocated to buildings. The use of fossil fuel for
650 building heating is extremely rare in Norway. The emissions in the “building” category in Norway are
651 mostly from light commercial activity: boilers, generators, ovens, and the similar emissions from light
652 commercial activity which are below the ETS reporting threshold. As discussed above, it is difficult to
653 characterize buildings (e.g. buildings as different as a hospital, mall, auto body shop, and small cottage
654 are not distinguishable, nor can mansions be differentiated from cottages) (Milojevic-Dupont et al.,
655 2020), but this is clearly a frontier where further work is merited.

656



657

658 *Figure 10: Example visualization of spatialized emissions inventory for Trondheim, a city of 200,000 in mid-Norway, and the*
659 *surrounding region. Small grey dots represent individual buildings; purple dots are emissions from fuel stations, and the large*
660 *orange dots are ETS-registered point source facilities (a waste incineration plant and a factory making mineral wool). This*
661 *detailed view, while only an estimate, can provide residents and government agencies a thought-provoking view of what*
662 *decarbonization will look like for their town.*

663

664

665 5. Code Availability

666 The source code not available at the time of writing. The authors plan to clean up the code and prepare
667 a publicly usable version in the future. This will be linked at the Zenodo data repository and project
668 home page.

669

670 6. Data Availability

671 Datasets are available via Zenodo at <https://doi.org/10.5281/zenodo.5482480> (Moran, 2021)

672 The Zenodo DOI is: 10.5281/zenodo.5482480



673 The model homepage, with an interactive map, is: <https://openghgmap.net>

674

675 **7. Limitations and Future Work**

676 One limitation of the approach presented in this paper, and a potential source of difficult-to-detect
677 bias, could be inconsistent coverage in OpenStreetMap. As OSM is a crowd-sourced dataset there is
678 no assurance of homogeneous coverage. Some areas of the country may be well-covered in OSM and
679 others only sparsely (Hecht et al., 2013). This could introduce biases such as underreporting the
680 number of fueling stations and thus underestimating vehicle traffic. The authors are not aware of any
681 effort to characterize the consistency of OSM coverage; this would be a valuable next step both for
682 the work presented here as well as for the OSM project and work derived therefrom.

683 For countries which do not participate in the ETS and do not have a similar domestic MRV system for
684 large point source carbon emitters, spatializing emissions from point source polluters will be a
685 challenge. Resources such as OSM and the Power Plant Database, which have considerable
686 information at the facility level (e.g. output in megawatts and fuel source for power plants), could be
687 of use.

688 The spatialization of emissions from vehicles and buildings - the two largest emissions categories - is
689 challenging. The assumption in ESCI that every fuel station serves an equal volume and mix of vehicles
690 is simplistic. The lack of even basic data characterizing buildings by height, area, age, or material,
691 makes it impossible to differentiate buildings as varied as a terrace house block, separated house,
692 mall, or hospital. Some novel approaches for characterizing building stocks have recently been
693 proposed (Haberl et al., 2021; Milojevic-Dupont et al., 2020; Peled and Fishman, 2021) which could be
694 used. Developing more accurate town-level models of building emissions may require different
695 modelling approaches, such as utilizing data from national building cadaster registries or from
696 advanced remote sensing datasets such as from synthetic aperture radar satellite constellations,
697 airborne LIDAR sensors, and machine learning used with mobile airborne or ground cameras.

698 Our emissions inventory can support local authorities in their journeys towards climate neutrality in
699 multiple manners. The inventory can help make local and regional sources of emissions more tangible
700 for diverse politicians, city administrations and local communities and provides a good starting point,
701 especially for communities that lack a detailed GHG emissions inventory. Making an abstract concept
702 such as greenhouse gas emissions more visible will enable discussions regarding localization and
703 upgrading of facilities and infrastructures and will provide a basis for emblematic changes with high
704 impact potential for the region. Connecting the inventory to digital urban twins with detailed
705 information regarding built environment characteristics, may help overcome the current limitations
706 of lack of building data.

707 In order to further develop the model, we will actively discuss and test it with local authorities to fine-
708 tune it to their needs in order to make informed decisions. Furthermore, we will explore how we can
709 further refine data collection, analysis and spatialization through the use of GIS combined with
710 crowdsourcing and citizen science.

711 To conclude, we present a new European emissions inventory which disaggregates national CO₂
712 inventories to city and county level administrative jurisdictions. The model is broadly consistent with
713 the ODIAC and EDGAR results but shows higher cell-level variability and provides results per-
714 jurisdiction rather than in a gridded form. The estimated inventories provided by this model can help
715 local governments begin establishing an emissions inventory.

716

717 **8. Author Contributions**



718 DM constructed the core model and led the manuscript writing. PP, HZ, HW, and JT contributed to the
719 results analysis. KRG contributed to the introduction literature review, and conceptual framework.
720 TW, AW contributed to the manuscript. HM, JK, DK, and AS contributed the aviation and marine
721 emissions modules of the model.

722

723 9. Acknowledgements

724 This work was conducted with support from the Norwegian Research Council under grant #
725 287690/F20.

726

727

728 10. References

- 729 Andres, R. J., Boden, T. A., and Marland, G.: Monthly Fossil-Fuel CO₂ Emissions: Mass of Emissions
730 Gridded by One Degree Latitude by One Degree Longitude, 10.3334/CDIAC/ffe.MonthlyMass.2016,
731 2016.
- 732 Andres, R. J., Marland, G., Fung, I., and Matthews, E.: A 1° × 1° distribution of carbon dioxide emissions
733 from fossil fuel consumption and cement manufacture, 1950-1990, 10.1029/96GB01523, 1996.
- 734 Asefi-Najafabady, S., Rayner, P. J., Gurney, K. R., McRobert, A., Song, Y., Coltin, K., Huang, J., Elvidge,
735 C., and Baugh, K.: A multiyear, global gridded fossil fuel CO₂ emission data product: Evaluation and
736 analysis of results, *Journal of Geophysical Research: Atmospheres*, 119, 10,213-210,231,
737 10.1002/2013JD021296, 2014.
- 738 Basu, S., Lehman, S. J., Miller, J. B., Andrews, A. E., Sweeney, C., Gurney, K. R., Xu, X., Southon, J., and
739 Tans, P. P.: Estimating US fossil fuel CO₂ emissions from measurements of C₁₄ in atmospheric CO₂,
740 *Proceedings of the National Academy of Sciences*, 117, 13300, 10.1073/pnas.1919032117, 2020.
- 741 Bun, R., Nahorski, Z., Horabik-Pyzel, J., Danylo, O., See, L., Charkovska, N., Topylko, P., Halushchak, M.,
742 Lesiv, M., Valakh, M., and Kinakh, V.: Development of a high-resolution spatial inventory of
743 greenhouse gas emissions for Poland from stationary and mobile sources, *Mitigation and Adaptation
744 Strategies for Global Change*, 24, 10.1007/s11027-018-9791-2, 2019.
- 745 Chen, G., Shan, Y., Hu, Y., Tong, K., Wiedmann, T., Ramaswami, A., Guan, D., Shi, L., and Wang, Y.:
746 Review on City-Level Carbon Accounting, 10.1021/acs.est.8b07071, 2019.
- 747 Davis, K. J., Deng, A., Lauvaux, T., Miles, N. L., Richardson, S. J., Sarmiento, D. P., Gurney, K. R.,
748 Hardesty, R. M., Bonin, T. A., Brewer, W. A., Lamb, B. K., Shepson, P. B., Harvey, R. M., Cambaliza, M.
749 O., Sweeney, C., Turnbull, J. C., Whetstone, J., and Karion, A.: The Indianapolis Flux Experiment
750 (INFLUX): A test-bed for developing urban greenhouse gas emission measurements, *Elementa*, 5,
751 10.1525/elementa.188, 2017.
- 752 Dijkstra, E. W.: A note on two problems in connexion with graphs, *Numerische Mathematik*, 1, 269
753 271, 10.1007/BF01386390, 1959.
- 754 Douglas, D. H. and Peucker, T. K.: ALGORITHMS FOR THE REDUCTION OF THE NUMBER OF POINTS
755 REQUIRED TO REPRESENT A DIGITIZED LINE OR ITS CARICATURE, *Cartographica: The International
756 Journal for Geographic Information and Geovisualization*, 10, 112-122, 10.3138/FM57-6770-U75U-
757 7727, 1973.
- 758 Fong, W. K., Sotos, M., Doust, M., Schultz, S., Marques, A., and Deng-Beck, C.: Global Protocol for
759 Community-Scale Greenhouse Gas Emission Inventories, WRI C40 Cities and ICLEI2016.
- 760 Gaughan, A. E., Oda, T., Sorichetta, A., Stevens, F. R., Bondarenko, M., Bun, R., Krauser, L., Yetman, G.,
761 and Nghiem, S. V.: Evaluating nighttime lights and population distribution as proxies for mapping
762 anthropogenic CO₂ emission in Vietnam, Cambodia and Laos, *Environmental Research
763 Communications*, 1, 091006, 10.1088/2515-7620/ab3d91, 2019.



- 764 Ghosh, S., Mueller, K., Prasad, K., and Whetstone, J.: Accounting for Transport Error in Inversions: An
765 Urban Synthetic Data Experiment, *Earth and Space Science*, 8, e2020EA001272,
766 <https://doi.org/10.1029/2020EA001272>, 2021.
- 767 Harris, S., Weinzettel, J., Bigano, A., and Källmén, A.: Low carbon cities in 2050? GHG emissions of
768 European cities using production-based and consumption-based emission accounting methods,
769 <https://doi.org/10.1016/j.jclepro.2019.119206>, 2020.
- 770 Hecht, R., Kunze, C., and Hahmann, S.: Measuring Completeness of Building Footprints in
771 OpenStreetMap over Space and Time, *ISPRS International Journal of Geo-Information*, 2,
772 10.3390/ijgi2041066, 2013.
- 773 IPCC: Guidelines for National Greenhouse Gas Inventories, Vol. 4, Chap. 4,
774 GOSAT-2 ESA Mission Homepage: <https://earth.esa.int/eogateway/missions/gosat-2>, last access:
775 August 23, 2021.
- 776 Jones, M., Andrew, R. M., Peters, G., Janssens-Maenhout, G., De-Gol, A., Ciais, P., Patra, P. K.,
777 Chevallier, F., and Le Quere, C.: Gridded fossil CO₂ emissions and related O₂ combustion consistent
778 with national inventories 1959–2018, *Scientific Data*, in press, 2020.
- 779 Kim, J., Shusterman, A. A., Lieschke, K. J., Newman, C., and Cohen, R. C.: The BERkeley Atmospheric
780 CO₂ Observation Network: field calibration and evaluation of low-cost air quality sensors, *Atmos.*
781 *Meas. Tech.*, 11, 1937–1946, 10.5194/amt-11-1937-2018, 2018.
- 782 Kona, A., Monforti-Ferrario, F., Bertoldi, P., Baldi, M. G., Kakoulaki, G., Vetter, N., Thiel, C., Melica, G.,
783 Lo Vullo, E., Sgobbi, A., Ahlgren, C., and Posnic, B.: Global Covenant of Mayors, a dataset of greenhouse
784 gas emissions for 6200 cities in Europe and the Southern Mediterranean countries, *Earth Syst. Sci.*
785 *Data*, 13, 3551–3564, 10.5194/essd-13-3551-2021, 2021.
- 786 Kurokawa, J., Ohara, T., Morikawa, T., Hanayama, S., Janssens-Maenhout, G., Fukui, T., Kawashima, K.,
787 and Akimoto, H.: Emissions of air pollutants and greenhouse gases over Asian regions during 2000–
788 2008: Regional Emission inventory in ASIA (REAS) version 2, *Atmospheric Chemistry and Physics*, 13,
789 11019–11058, 10.5194/acp-13-11019-2013, 2013.
- 790 Lauvaux, T., Gurney, K. R., Miles, N. L., Davis, K. J., Richardson, S. J., Deng, A., Nathan, B. J., Oda, T.,
791 Wang, J. A., Hutyra, L., and Turnbull, J.: Policy-Relevant Assessment of Urban CO₂ Emissions,
792 10.1021/acs.est.0c00343, 2020.
- 793 Long, Z., Zhang, Z., Liang, S., Chen, X., Ding, B., Wang, B., Chen, Y., Sun, Y., Li, S., and Yang, T.: Spatially
794 explicit carbon emissions at the county scale, *Resources, Conservation and Recycling*, 173, 105706,
795 <https://doi.org/10.1016/j.resconrec.2021.105706>, 2021.
- 796 Mallia, D. V., Mitchell, L. E., Kunik, L., Fasoli, B., Bares, R., Gurney, K. R., Mendoza, D. L., and Lin, J. C.:
797 Constraining Urban CO₂ Emissions Using Mobile Observations from a Light Rail Public Transit Platform,
798 *Environmental Science & Technology*, 54, 15613–15621, 10.1021/acs.est.0c04388, 2020.
- 799 Meng, L., Graus, W., Worrell, E., and Huang, B.: Estimating CO₂ (carbon dioxide) emissions at urban
800 scales by DMSP/OLS (Defense Meteorological Satellite Program's Operational Linescan System)
801 nighttime light imagery: Methodological challenges and a case study for China, *Energy*, 71, 468–478,
802 10.1016/j.energy.2014.04.103, 2014.
- 803 Moran, D.: OpenGHGMap - Europe - CO₂ Emissions in 108,000 European Cities (2018_20210907a)
804 (2018_20210907a) [dataset], [10.5281/zenodo.5482480](https://doi.org/10.5281/zenodo.5482480), 2021.
- 805 Mueller, K. L., Lauvaux, T., Gurney, K. R., Roest, G., Ghosh, S., Gourdji, S. M., Karion, A., DeCola, P., and
806 Whetstone, J.: An emerging GHG estimation approach can help cities achieve their climate and
807 sustainability goals, *Environmental Research Letters*, 16, 084003, 10.1088/1748-9326/ac0f25, 2021.
- 808 Nangini, C., Peregón, A., Ciais, P., Weddige, U., Vogel, F., Wang, J., Bron, F.-M., Bachra, S., Wang, Y.,
809 Gurney, K., Yamagata, Y., Appleby, K., Telahoun, S., Canadell, J. G., Grbler, A., Dhakal, S., and Creutzig,
810 F.: A global dataset of CO₂ emissions and ancillary data related to emissions for 343 cities, *Scientific*
811 *Data*, 6, 180280, 10.1038/sdata.2018.280, 2019.
- 812 NASA OCO-2 Mission Homepage: https://www.nasa.gov/mission_pages/oco2/index.html, last access:
813 August 23, 2021.



- 814 Nassar, R., Napier-Linton, L., Gurney, K. R., Andres, R. J., Oda, T., Vogel, F. R., and Deng, F.: Improving
815 the temporal and spatial distribution of CO₂ emissions from global fossil fuel emission data sets,
816 10.1029/2012JD018196, 2013.
- 817 Osses, M., Rojas, N., Ibarra, C., Valdebenito, V., Laengle, I., Pantoja, N., Osses, D., Basoa, K., Tolvett, S.,
818 Huneeus, N., Gallardo, L., and Gómez, B.: High-definition spatial distribution maps of on-road
819 transport exhaust emissions in Chile, 1990 - 2020, *Earth Syst. Sci. Data Discuss.*, 2021, 1-27,
820 10.5194/essd-2021-218, 2021.
- 821 Ramaswami, A. and Chavez, A.: What metrics best reflect the energy and carbon intensity of cities?
822 Insights from theory and modeling of 20 US cities, *Environmental Research Letters*, 8, 035011,
823 10.1088/1748-9326/8/3/035011, 2013.
- 824 Ramer, U.: An iterative procedure for the polygonal approximation of plane curves, *Computer
825 Graphics and Image Processing*, 1, 244-256, [https://doi.org/10.1016/S0146-664X\(72\)80017-0](https://doi.org/10.1016/S0146-664X(72)80017-0), 1972.
- 826 Rayner, P. J., Raupach, M. R., Paget, M., Peylin, P., and Koffi, E.: A new global gridded data set of CO₂
827 emissions from fossil fuel combustion: Methodology and evaluation, 10.1029/2009JD013439, 2010.
- 828 Shan, Y., Guan, D., Liu, J., Mi, Z., Liu, Z., Liu, J., Schroeder, H., Cai, B., Chen, Y., Shao, S., and Zhang, Q.:
829 Methodology and applications of city level CO₂ emission accounts in China, *Journal of Cleaner
830 Production*, 161, 1215-1225, <https://doi.org/10.1016/j.jclepro.2017.06.075>, 2017.
- 831 Shan, Y., Guan, D., Hubacek, K., Zheng, B., Davis, S. J., Jia, L., Liu, J., Liu, Z., Fromer, N., Mi, Z., Meng, J.,
832 Deng, X., Li, Y., Lin, J., Schroeder, H., Weisz, H., and Schellnhuber, H. J.: City-level climate change
833 mitigation in China, 10.1126/sciadv.aaq0390, 2018.
- 834 Turnbull, J. C., Karion, A., Davis, K. J., Lauvaux, T., Miles, N. L., Richardson, S. J., Sweeney, C., McKain,
835 K., Lehman, S. J., Gurney, K. R., Patarasuk, R., Liang, J., Shepson, P. B., Heimbürger, A., Harvey, R., and
836 Whetstone, J.: Synthesis of Urban CO₂ Emission Estimates from Multiple Methods from the
837 Indianapolis Flux Project (INFLUX), *Environmental Science & Technology*, 53, 287-295,
838 10.1021/acs.est.8b05552, 2019.
- 839 Wang, R., Tao, S., Ciais, P., Shen, H. Z., Huang, Y., Chen, H., Shen, G. F., Wang, B., Li, W., Zhang, Y. Y.,
840 Lu, Y., Zhu, D., Chen, Y. C., Liu, X. P., Wang, W. T., Wang, X. L., Liu, W. X., Li, B. G., and Piao, S. L.: High-
841 resolution mapping of combustion processes and implications for CO₂ emissions,
842 10.5194/acp-13-5189-2013, 2013.
- 843 Whetstone, J. R.: Advances in urban greenhouse gas flux quantification: The Indianapolis Flux
844 Experiment (INFLUX), *Elementa: Science of the Anthropocene*, 6, 10.1525/elementa.282, 2018.
- 845 Wu, D., Lin, J. C., Oda, T., and Kort, E. A.: Space-based quantification of per capita CO₂ emissions from
846 cities, *Environmental Research Letters*, 15, 035004, 10.1088/1748-9326/ab68eb, 2020.
- 847 Yanto, J. and Liem, R. P.: Aircraft fuel burn performance study: A data-enhanced modeling approach,
848 *Transportation Research Part D: Transport and Environment*, 65, 574-595,
849 <https://doi.org/10.1016/j.trd.2018.09.014>, 2018.
- 850 Zheng, B., Cheng, J., Geng, G., Wang, X., Li, M., Shi, Q., Qi, J., Lei, Y., Zhang, Q., and He, K.: Mapping
851 anthropogenic emissions in China at 1 km spatial resolution and its application in air quality modeling,
852 *Science Bulletin*, 66, 612-620, <https://doi.org/10.1016/j.scib.2020.12.008>, 2021.

853